

Impact of EDGES 21cm Global Signal on Primordial Power Spectrum

Shintaro Yoshiura ^a, Keitaro Takahashi ^a, and Tomo Takahashi ^b

^a*Faculty of Advanced Science and Technology, Kumamoto University, Kumamoto, Japan*

^b*Department of Physics, Saga University, Saga 840-8502, Japan*

Abstract

We investigate the impact of the recent observation of the 21cm global signal by EDGES on primordial power spectrum, particularly focusing on the running parameters α_s and β_s which characterize the detailed scale dependence of the primordial spectrum. When primordial power spectrum is enhanced/suppressed on small scales, the structure formation proceeds faster/slower and changes the abundance of small size halos, which affects the sources of Lyman α radiation at high redshifts to alter the position of the absorption line. Recent observation of EDGES detected the 21cm absorption line at $z = 17.2$ and this result also indicates that the brightness temperature is consistent with zero for $z \lesssim 14$ and $z \gtrsim 22$, which can exclude a scenario giving the absorption line at such redshifts. We argue that the bound on the running parameters can be obtained by requiring that the absorption line should not exceed observational bounds at such redshift ranges and found that some parameter space of α_s and β_s allowed by Planck may be disfavored for some values of astrophysical parameters.

1 Introduction

The nature of primordial fluctuations reflects the physical mechanism behind the inflationary Universe and hence a great deal of effort has been made to understand it both from observational and theoretical viewpoints. Current cosmological observations such as cosmic microwave background (CMB) from Planck satellite have measured primordial power spectrum, in particular, its amplitude and the spectral index n_s very accurately [1, 2], and together with the bound on the amplitude of primordial gravitational waves such as from CMB B-mode observations like BICEP2/KECK [3], the inflationary models are now severely tested. Nevertheless there remains a large variety of inflationary models consistent with those observations and we are still far from a thorough understanding of the inflationary Universe. Therefore it is imperative to go further to probe primordial fluctuations.

One direction would be to measure the primordial power spectrum more precisely. For this purpose, it is common to adopt the following parametrization for the primordial spectrum:

$$P_\zeta(k) = A_s(k_{\text{ref}}) \left(\frac{k}{k_{\text{ref}}} \right)^{n_s - 1 + \frac{1}{2}\alpha_s \ln(k/k_{\text{ref}}) + \frac{1}{3!}\beta_s \ln^2(k/k_{\text{ref}})}, \quad (1.1)$$

where $A_s(k_{\text{ref}})$ is the amplitude at the reference scale k_{ref} , n_s is the spectral index. α_s and β_s are the so-called running parameters and represent the detailed scale dependence of $P_\zeta(k)$ as

$$\alpha_s = \left. \frac{d^2 \ln P_\zeta(k)}{d \ln k^2} \right|_{k=k_{\text{ref}}}, \quad \beta_s = \left. \frac{d^3 \ln P_\zeta(k)}{d \ln k^3} \right|_{k=k_{\text{ref}}}. \quad (1.2)$$

Although one can obtain the bounds on the running parameters from Planck data, they are not so severe and thus it is worth exploring a possibility of probing the runnings by using yet another observation to measure them more accurately.

When one wishes to determine the runnings precisely, probing the power spectrum on a wide range of scales would be helpful. Since CMB measures cosmic fluctuations on large scales, one needs observations on small scales. As such, expected constraints from future observations of 21cm fluctuations of neutral hydrogen from intergalactic medium [4, 5] and minihalos [6], and CMB spectral μ distortions^{#1} [7–10] have been studied.

We in this paper investigate how the nature of primordial power spectrum affects the 21cm global signal and the impact of the recent EDGES result [17] on the running parameters. EDGES has reported that the absorption peak is observed at the frequency corresponding to $z = 17.2$ and its brightness temperature relative to CMB is $T_b = -500_{-500}^{+200}$ mK (99% C.L.), whose value is too low to be explained in the standard cosmological and astrophysical scenarios^{#2}. This result has stimulated many works which aim to explain its non-standard value by resorting to dark matter (DM) interactions to cool the gas (baryon) [19–26], which could be confronted with other cosmological/astrophysical observations [27–29]. Other possibilities

^{#1} In addition to the μ distortion [11–15], the i -distortion [16] can also give a useful information on primordial power spectrum.

^{#2} See, however, Ref. [18] for the discussion on the analysis and its interpretation.

to explain the signal have been discussed in models with producing photons at radio wavelength [30–36], dark sector properties [37–39] and so on. On the other hand, there have been several works to derive constraints on DM and primordial black holes by using the EDGES result [40–49]. Implications of the EDGES result for 21cm power spectrum have also been investigated [50, 51].

One should notice that the EDGES result also indicates that there is no absorption signal at the redshift regions $z \lesssim 14$ and $z \gtrsim 22$, which can constrain the running parameters of primordial power spectrum. Since the runnings α_s and β_s directly affect the matter power on small scales, the structure formation should change depending on these parameters. For too positively (negatively) large values of α_s and β_s , the matter power on small scales are enhanced (suppressed) and the structure formation is affected. When the structure formation proceeds faster (slower) due to the enhanced (suppressed) matter power spectrum on small scales, which switches on the source of Lyman α radiations earlier (later), then the absorption line is shifted to a higher (lower) redshift^{#3}. If the absorption line appears at the redshift ranges $z \lesssim 14$ or $z \gtrsim 22$, it is inconsistent with the EDGES result and such parameter values are disfavored. By adopting this argument, we can obtain the bound on the running parameters α_s and β_s from EDGES, which is the main purpose of this paper.

The organization of this paper is the following. In the next section, we briefly describe the procedure to compute the 21cm brightness temperature and discuss the effects of the runnings on the global signal of 21cm line. Then in Section 3, we investigate the bound on the running parameters from EDGES by requiring that the absorption line should not appear at the redshift ranges $z \lesssim 14$ and $z \gtrsim 22$. The effects of astrophysical parameters on the 21cm global signal and constraints on the running parameters are discussed in Section 4. The final section is devoted to conclusion of this paper.

2 21cm global signal and primordial power spectrum

Here we briefly discuss how the nature of primordial power spectrum affects the global signal of 21cm line of neutral hydrogen.

The 21cm global signal, averaged differential brightness temperature relative to CMB radiation, is given by [53–55] (see, e.g., the reviews [56, 57])

$$T_b \simeq 27 x_{\text{HI}} \left(\frac{\Omega_b h^2}{0.023} \right) \left(\frac{0.15}{\Omega_m h^2} \right)^{1/2} \left(\frac{1+z}{10} \right)^{1/2} \left(\frac{T_s - T_{\text{CMB}}}{T_s} \right) \text{mK}, \quad (2.3)$$

where Ω_b, Ω_m are density parameters for baryon and (total) matter, h is the Hubble parameter in units of $100 \text{ km s}^{-1} \text{ Mpc}^{-1}$, T_s is the spin temperature of neutral hydrogen, $T_{\text{CMB}} = 2.725/(1+z)$ is the temperature of CMB photon. The spin temperature T_s can be

^{#3} When the running parameters are too negative where the matter power on small scales is suppressed, its effects are similar to the case with warm dark matter [47, 52].

given by

$$T_s^{-1} = \frac{T_{\text{CMB}}^{-1} + x_\alpha T_\alpha^{-1} + x_c T_K^{-1}}{1 + x_\alpha + x_c}, \quad (2.4)$$

where T_α and T_K respectively are the color temperature and gas temperature, respectively. x_α and x_c are the coupling coefficients characterizing the scattering of Lyman α photons and the atomic collisions. For the detailed discussion of the evolution of the spin temperature, see e.g., Refs. [56, 57].

To investigate how the running parameters α_s and β_s affect the brightness temperature, we have computed the evolution of the spin temperature by using 21cmFAST [58, 59]. To calculate its evolution, we also need to specify astrophysical parameters such as the minimum virial temperature of star forming sources T_{vir} , the fraction of baryons converted to stars f_* and the number of X-ray photons emitted from stars ζ_X . The evolution of the spin temperature is also sensitive to these astrophysical parameters^{#4}. We discuss how these parameters affects the absorption line in Section 4.

In Fig. 1, we show the evolutions of T_s, T_K and T_{CMB} (left panel) and the differential brightness temperature T_b (right panel) for several parameter sets of (n_s, α_s, β_s) , whose values are indicated in the figure. The astrophysical parameters mentioned above are assumed as $T_{\text{vir}} = 10^4$ K, $f_* = 0.05$ and $\zeta_X = 2 \times 10^{56}/M_\odot$. The cosmological parameters are taken as follows: $\sigma_8 = 0.831$, $\Omega_b h^2 = 0.02225$, $\Omega_m = 0.3156$, $h = 0.6727$ where σ_8 is the amplitude of matter fluctuations at $8h^{-1}$ Mpc. As mentioned in the introduction, when α_s and β_s are positively (negatively) large, the matter power on small scales are enhanced (suppressed), and thus the structure formation proceeds faster (slower) and the sources of Lyman α background are switched on earlier (later). Therefore positively (negatively) larger values of α_s and β_s drive the spin temperature to approach the gas temperature earlier (later), which shifts the absorption line to a higher (lower) redshift. On the other hand, the recent EDGES result indicates that the absorption line appears at around $z = 17.2$ and the brightness temperature goes to zero for $z \lesssim 14$ and $z \gtrsim 22$, therefore too large positive or negative values of the runnings are expected to be disfavored in the light of recent EDGES result. In the next section, we investigate the bound on the runnings α_s and β_s from the requirement that the redshift (frequency) of the absorption line should be consistent with the EDGES result, i.e., it should not appear at $z \lesssim 14$ and $z \gtrsim 22$.

^{#4} In 21cmFAST, the evolution of the spin temperature is solved with semi-analytic models and approximations such as the one regarding the characterization of X-ray sources and a step function for the optical depth. The accuracy of ionization model has been investigated in [59, 60], and the power spectrum matches with the numerical simulation within 10% of error. However, the accuracy of 21cmFAST for the global signal has not been discussed, and one has to perform a massive radiative transfer simulation and 21cmFAST with the same initial condition to validate its accuracy. This is outside the scope of this paper. However, it should be mentioned that the entire evolution of the global signal is fairly consistent with the results obtained by using independent semi-numerical simulations (e.g. [61, 62]) and radiative transfer simulations (e.g. [63, 64]).

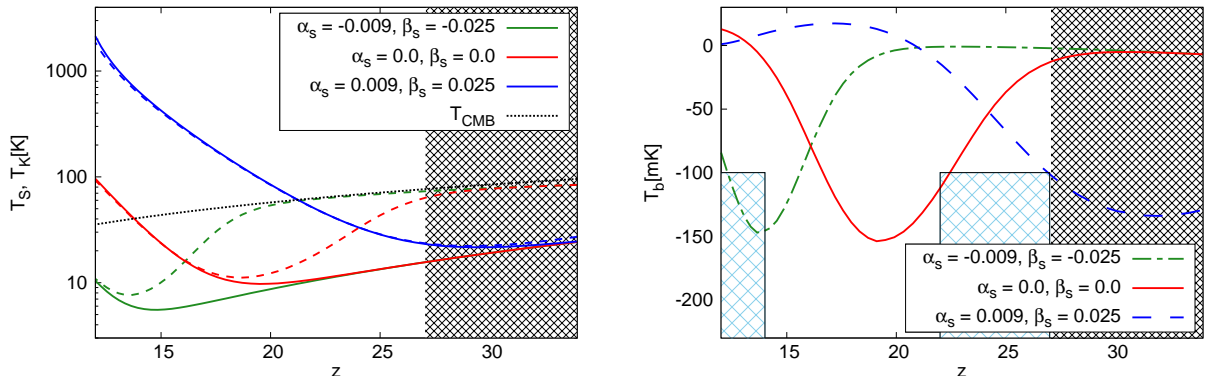


Figure 1: [Left panel]: Evolution of T_k (solid), T_s (dashed) and T_{CMB} (dotted). [Right panel]: Evolution of the brightness temperature T_b . Cases with $(n_s, \alpha_s, \beta_s) = (0.9586, 0, 0)$ (red), $(0.9586, 0.009, 0.025)$ (blue) and $(0.9586, -0.009, -0.025)$ (green) are shown. Light blue hatched regions correspond to the ones inconsistent with the EDGES result. Black hatched one indicates that there is no data in the redshift range.

3 Bounds on primordial power spectrum from EDGES 21cm global signal

Now in this section, we study the bound on the running parameters α_s and β_s of primordial power spectrum by demanding that the absorption line should appear in the redshift range of $14 < z < 22$ indicated by the EDGES result. In practice, we conservatively require that the brightness temperature should be $T_b > -100$ mK for the redshift range $z < 14$ and $z > 22$. We note that, since EDGES does not give data for $z \gtrsim 27$, we do not constrain the case where the absorption trough appears at redshifts $z > 27$.

In Fig. 2, color panels of the redshift of the peak position of the absorption trough z_{peak} and allowed region from EDGES are shown in the α_s - β_s plane. To obtain a constraint from EDGES, we basically only use the information of the position of the absorption trough (not of the amplitude). As mentioned, the EDGES result indicates that the absorption line should appear in the redshift range of $14 < z < 22$. We define a criterion for the allowed model such that the absorption line fall into this redshift range. To be precise, for the allowed model, we require that the predicted evolution of T_b does not cross the blue hatched regions in the right panel of Fig. 1, where we conservatively demand that $T_b > -100$ mK even for $z < 14$ and $z > 22$, taking observational errors into account. Since there is no data for $z > 27$ and $z < 13.2$, when the peak of the absorption trough is $z > 27$ or $z < 13.2$, we cannot obtain any constraint, which is shown as “Not constrained (no data)” in the figure. We consider a flat Λ CDM model and fixed other cosmological parameters as $\sigma_8 = 0.831, \Omega_b h^2 = 0.02225, \Omega_m = 0.3156, h = 0.6727$ as assumed in Fig. 1 since these parameters are well measured by Planck [1]. By doing so in the analysis, we effectively combine the Planck results with the 21cm global signal by EDGES. Regarding the spectral

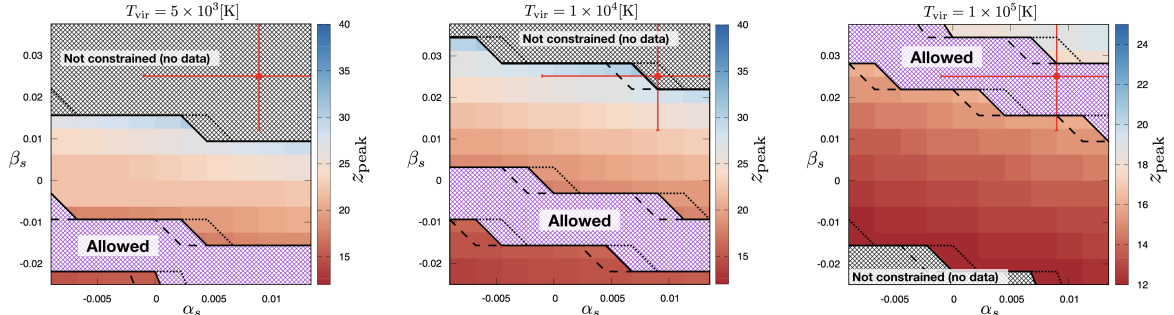


Figure 2: Allowed region from the EDGES result and the peak redshift of the absorption trough z_{peak} are shown with a color panel for the cases with $T_{\text{vir}} = 5 \times 10^3$ K (left), 10^4 K (middle) and 10^5 K (right). Other cosmological and astrophysical parameters are fixed as described in the text. Here n_s is fixed to be $n_s = 0.9530, 0.9586$ and 0.9642 which correspond to the values of 1σ lower, central and 1σ upper bound from Planck and depicted as dotted, solid and dashed lines, respectively. Red point shows Planck best fit value with 1 sigma error bars. When the peak redshift of the absorption line is in the range of $z > 27$ or $T_b > -100$ mK at $z = 27$, no constraint can be obtained from EDGES, which is indicated by black hatched. It should be noted that the constraint depends on the values of astrophysical parameters, which will be discussed in Section 4.

index n_s , its effect on the brightness temperature is degenerate with the running parameters α_s and β_s , and hence we take $n_s = 0.9530, 0.9586$ and 0.9642 which are respectively the values of 1σ lower, central and 1σ upper bound from Planck [2], and respectively depicted with dotted, solid and dashed lines in Fig. 2. As seen from the figure, the change of n_s within the 1σ range allowed by Planck does not affect the constraint on α_s and β_s much. For astrophysical parameters, we take $T_{\text{vir}} = 5 \times 10^3$ K (left), 10^4 K (middle) and 10^5 K (right). Other astrophysical parameters are assumed as $f_* = 0.05$ and $\zeta_X = 2 \times 10^{56}/M_\odot$. With this value of ζ_X , 0.3 X-ray photons are emitted per stellar baryon.

Since large positive and negative values of α_s and β_s give too high or too low redshift of the absorption trough as discussed in the previous section, such regions can be considered to be excluded by the EDGES result. We note that the constraints on α_s and β_s derived from Planck 2015 TT, TE, EE+lowP analysis are [2]

$$\alpha_s = 0.009 \pm 0.010, \quad \beta_s = 0.025 \pm 0.013, \quad (3.5)$$

which is also indicated in Fig 2.

Although constraints on α_s and β_s depend on the values of astrophysical parameters such as T_{vir} as shown in Fig. 2, it is interesting to see that some parameter region for α_s and β_s

allowed by Planck at 1σ can be ruled out by the EDGES for some values of T_{vir} . This shows that the 21cm global signal is powerful in constraining the runnings of primordial power spectrum although some of the parameter space cannot be constrained since the EDGES measures the redshift range of $14 \lesssim z \lesssim 27$. We should also note that, although the recent result from EDGES may need to be confirmed by other observations of the 21cm global signal, as far as the frequency range of the absorption trough persists (even if the size of the absorption signal is weakened), the constraint obtained in this paper will still be valid.

As mentioned above, the constraint on the running parameters depend on the astrophysical parameters such as T_{vir} . In the next section, we discuss effects of the astrophysical parameters on the evolution of the brightness temperature and how the constraint is affected in some detail.

4 Effects of Astrophysical Parameters

As discussed in the previous section, our analysis indicates that some parameter space of α_s and β_s allowed by Planck could be disfavored by the EDGES result for some fixed astrophysical parameters. However, the 21cm global signal also strongly depends on the astrophysical parameters used in 21cmFAST. Here we discuss in some detail how the astrophysical parameters such as T_{vir} , f_* and ζ_X affect the 21cm absorption signal^{#5}.

In Fig. 3, we show the evolution of the brightness temperature T_b by varying the values of T_{vir} (top panel), f_* (middle panel) and ζ_X (bottom panel). Since T_{vir} and f_* affect the WF coupling and gas heating in the same way, the effects of these parameters on the 21cm global signal are degenerate. But on the other hand, ζ_X only affects gas heating, and hence the variation of ζ_X is not degenerate with the other parameters.

Concerning T_{vir} , a negative feedback effect such as Lyman-Werner radiation at high redshifts leads to the suppression of the star formation in halos [65], which results in a larger value of T_{vir} and the reduction of X-ray and Lyman- α photons from small halos, then the absorption line shifts to a lower redshift. The fraction of baryon converted to stars f_* also alters the number of X-ray and Lyman- α photons. Smaller values of f_* make the WF coupling less effective at higher redshifts and gas heating occur later, and thus the absorption peak shifts to a lower redshift, whose effect is quite similar to the one for T_{vir} . Therefore, as can be seen from Fig. 3, the change in T_{vir} and f_* give a degenerate effect on the evolution of T_b .

In Fig. 4, to see how the values of T_{vir} affects the constraints on the running parameters, we show constraints on the α_s - T_{vir} (left) and β_s - T_{vir} (right) planes with the other running parameter fixed as $\beta_s = 0.025$ (left) and $\alpha_s = 0.009$ (right) which corresponds to the central values derived from Planck [2]. As seen from the left panel, the constraint on α_s is not much

^{#5} Another parameter such as the ionizing efficiency ζ can also affect the 21cm signal. However, we note that the ionization starts after X-ray heating with our choice of the parameters such as the ionizing efficiency $\zeta = 20$ and $\zeta_X = 2 \times 10^{56}/M_\odot$. Furthermore, models with the high ionization rate are ruled out by the constraint of Thomson scattering optical depth of the CMB. Thus, these parameters may not change the results.

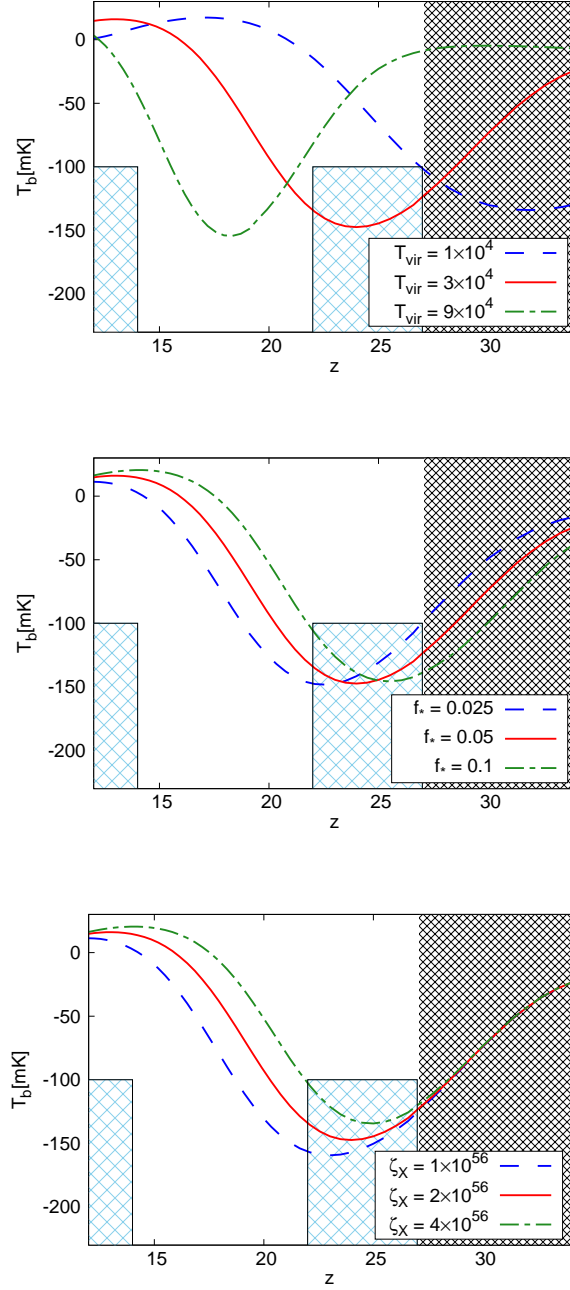


Figure 3: Evolution of the brightness temperature for various sets of astrophysical parameters. We show the impact of minimum virial temperature, T_{vir} (top), fraction of baryon converted to stars, f_* (middle) and X-ray heating efficiency, ζ_X (bottom). Here we assume $n_s = 0.9586$, $\alpha_s = 0.009$, $\beta_s = 0.025$ for the spectral index and its runnings. Light blue hatched regions correspond to the ones inconsistent with the EDGES result. Black hatched one indicates that there is no data in the redshift range.

affected by the value of T_{vir} . This also suggests that other cosmological parameters such as f_* and ζ_X do not affect the constraint on α_s much. On the other hand, the constraint on β_s is much affected by the value of T_{vir} assumed. As discussed above, larger value of T_{vir} shifts the absorption line to lower redshift, and hence larger T_{vir} allows more positive values of β_s . However, we should note that when $T_{\text{vir}} \lesssim 5 \times 10^4$ K, the EDGES result indicates $\beta_s \lesssim 0.012$ which means that the Planck allowed region may be disfavored for $T_{\text{vir}} \lesssim 5 \times 10^4$ K.

Although the constraints on β_s and T_{vir} are degenerate from EDGES data, measurements of faint galaxies at high- z would be useful to resolve the degeneracy between β_s and T_{vir} . For example, based on massive data of Hubble Space Telescope (HST), faint end magnitude of UV luminosity function is -18 at $z = 8$ [66], which corresponds to $T_{\text{vir}} \simeq 2 \times 10^5$ [K] [67]. Furthermore, the gravitational lensing method can help to find much fainter galaxies [68]. Meanwhile, the James Webb Space Telescope (JWST) is supposed to launch in 2021 and expected to find fainter galaxies [69]. Thus, T_{vir} will be constrained by combining the gravitational lensing method and the JWST. In distant future, $T_{\text{vir}} = 10^4$ [K], corresponding to atomic cooling, might be constrained by next generation telescopes such as the High Definition Space Telescope [70] and the Advanced Technology Large Aperture Space Telescope [71].

Although we only show the figures in the α_s - T_{vir} and β_s - T_{vir} planes, one can also infer the effects of other astrophysical parameters on the constraints on the running parameters. For example, due to the degeneracy between T_{vir} and f_* , if f_* is assumed to be smaller than $f_* = 0.05$ which is the fiducial value in our analysis, the allowed region of β_s would be shifted to the direction of larger β_s .

Regarding ζ_X , since the number of X-ray photons emitted from stars ζ_X affects gas heating, but not the WF coupling, the evolution of T_b at high redshift is not much affected by the change in ζ_X as seen from the bottom panel of Fig. 3. At lower redshift, the change of ζ_X gives a different efficiency of gas heating, which affects the lower part of the absorption trough. For example, by assuming a smaller value for ζ_X , T_b gets cooler due to less heating, which shifts the peak redshift of the absorption line to a lower one. Therefore, with smaller ζ_X , only the lower bound of the constraint on α_s and β_s would be shifted to more larger values, while the upper bounds are unaffected. On the other hand, powerful heating due to the higher value of ζ_X can increase T_b at lower redshifts. We also note that ζ_X affects the ionization history, it would give a very important effect when we look at lower redshift as $z \lesssim 10$, which however is not important in the redshift range we consider in this paper.

Here we should also mention that there are other parameters which affect the X-ray heating, such as the minimum energy of X-ray heating, E_0 , and the spectral index of X-ray radiation, α_X . Effects of these parameters on the behavior of 21cm global signal have been discussed in [72], from which one can see that their impact on the evolution of T_b is similar to the one by ζ_X , but weaker than ζ_X . Thus, we do not show the dependence of 21cm global signal on E_0 and α_X here.

Before closing this section, we make a comment on a possibility of constraining primordial power spectrum from the 21cm global signal at lower redshifts. The running parameters can also be constrained via the information of the signal at lower redshifts, especially from the argument of the ionization history. However, the evolution of ionization fraction depends

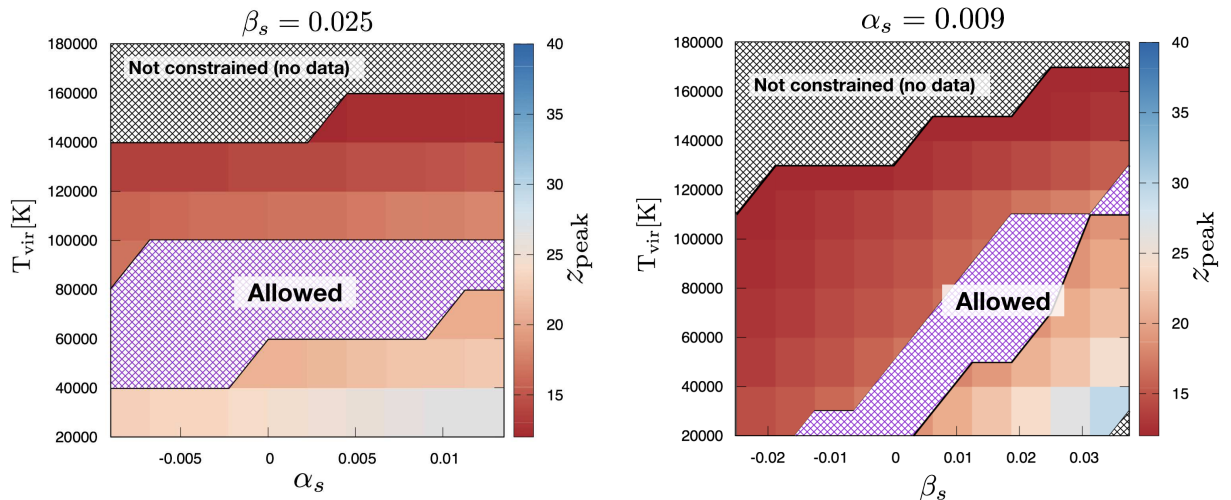


Figure 4: Allowed region from the EDGES result and the peak redshift of the absorption trough z_{peak} are shown with a color panel in the α_s - T_{vir} (left) and β_s - T_{vir} (right) planes. For the left and right panels, we fix the other running parameter as $\beta_s = 0.025$ (left) and $\alpha_s = 0.009$ (right). Other cosmological and astrophysical parameters are fixed as in Fig. 2. In the right panel, although the allowed region is disconnected at around $(\beta_s, T_{\text{vir}}) \sim (0.03, 1.1 \times 10^5 \text{ [K]})$, this is due to sparse grid sampling in the analysis. Since β_s and T_{vir} are degenerate, the allowed regions should be connected if we adopt denser sampling.

on other additional parameters such as the escape fraction of ionizing photon, ionization efficiency, maximum mean free path of ionizing photon and T_{vir} during the EoR era^{#6}. It would be worth investigating an attainable constraint on the running parameters by using the information at such lower redshifts. However, we need to take account of the effect of various astrophysical parameters mentioned above, which is computationally very demanding. We leave this for future work.

5 Conclusion

We have investigated the impact of the recent EDGES result on primordial power spectrum, particularly focusing on the running parameters α_s and β_s . EDGES has detected the absorption line at the frequency corresponding to $z = 17.2$ and also indicates that the absorption line should not appear in the redshift range of $z < 14$ and $z > 22$. Since large values of the runnings α_s and β_s directly enhance/suppress the matter power on small scales, the process of the structure formation is much affected, which changes the position of the absorption

^{#6} For a work on constraints on ionization history at low-redshift motivated by the EDGES result, see [73].

trough of the 21cm global signal. By requiring that the absorption line should appear at the frequency consistent with the EDGES result, we have obtained the bounds on the running parameters α_s and β_s . In particular, for some values of astrophysical parameters such as T_{vir} , f_* and ζ_X , the parameter space of α_s and β_s allowed by Planck can be excluded in the light of the EDGES result.

Since the absorption line detected by EDGES was somewhat unexpected, and hence further analysis with other instruments will be awaited to draw a more rigorous conclusion regarding constraints on primordial power spectrum. Especially, more systematic analysis for foreground removal would be inevitable. However, as our analysis demonstrates that the 21cm global signal is very powerful in constraining primordial power spectrum, future observational/theoretical studies of the 21cm global signal would bring us more insight to understand the primordial Universe.

Note added: After the submission of this manuscript, Planck made the final data release [74, 75], in which constraints on the running parameters are given by

$$\alpha_s = 0.013 \pm 0.012 (0.002 \pm 0.010), \quad \beta_s = 0.022 \pm 0.012 (0.010 \pm 0.013), \quad (5.6)$$

from the data set of Planck 2018 TT(TT, TE, EE)+lowE+lensing [75]. Although these values are slightly different from Planck 2015 result which we mentioned in the main text, our arguments remain unchanged.

Acknowledgments

We would like to thank Bradley Greig for helpful comments on the performance of the 21cm-FAST. This work is partially supported by JSPS KAKENHI Grant Number 15K05084 (TT), 16H05999 (KT), 16J01585 (SY), 17H01110 (KT), 17H01131 (TT), MEXT KAKENHI Grant Number 15H05888 (TT), 15H05896 (KT), and Bilateral Joint Research Projects of JSPS (KT).

References

- [1] P. A. R. Ade *et al.* [Planck Collaboration], *Astron. Astrophys.* **594**, A13 (2016) [arXiv:1502.01589 [astro-ph.CO]].
- [2] P. A. R. Ade *et al.* [Planck Collaboration], *Astron. Astrophys.* **594**, A20 (2016) [arXiv:1502.02114 [astro-ph.CO]].
- [3] P. A. R. Ade *et al.* [BICEP2 and Keck Array Collaborations], *Phys. Rev. Lett.* **116**, 031302 (2016) [arXiv:1510.09217 [astro-ph.CO]].
- [4] K. Kohri, Y. Oyama, T. Sekiguchi and T. Takahashi, *JCAP* **1310**, 065 (2013) [arXiv:1303.1688 [astro-ph.CO]].

- [5] J. B. Muñoz, E. D. Kovetz, A. Raccanelli, M. Kamionkowski and J. Silk, *JCAP* **1705**, 032 (2017) [arXiv:1611.05883 [astro-ph.CO]].
- [6] T. Sekiguchi, T. Takahashi, H. Tashiro and S. Yokoyama, *JCAP* **1802**, no. 02, 053 (2018) [arXiv:1705.00405 [astro-ph.CO]].
- [7] J. B. Dent, D. A. Easson and H. Tashiro, *Phys. Rev. D* **86**, 023514 (2012) [arXiv:1202.6066 [astro-ph.CO]].
- [8] R. Khatri and R. A. Sunyaev, *JCAP* **1306**, 026 (2013) [arXiv:1303.7212 [astro-ph.CO]].
- [9] G. Cabass, A. Melchiorri and E. Pajer, *Phys. Rev. D* **93**, no. 8, 083515 (2016) [arXiv:1602.05578 [astro-ph.CO]].
- [10] K. Kainulainen, J. Leskinen, S. Nurmi and T. Takahashi, *JCAP* **1711**, no. 11, 002 (2017) [arXiv:1707.01300 [astro-ph.CO]].
- [11] R. A. Sunyaev and Y. B. Zeldovich, *Astrophys. Space Sci.* **7**, 20 (1970).
- [12] W. Hu and J. Silk, *Phys. Rev. D* **48**, 485 (1993).
- [13] J. Chluba and R. A. Sunyaev, *Mon. Not. Roy. Astron. Soc.* **419**, 1294 (2012) [arXiv:1109.6552 [astro-ph.CO]].
- [14] J. Chluba, R. Khatri and R. A. Sunyaev, *Mon. Not. Roy. Astron. Soc.* **425**, 1129 (2012) [arXiv:1202.0057 [astro-ph.CO]].
- [15] R. Khatri, R. A. Sunyaev and J. Chluba, *Astron. Astrophys.* **543**, A136 (2012) [arXiv:1205.2871 [astro-ph.CO]].
- [16] R. Khatri and R. A. Sunyaev, *JCAP* **1209**, 016 (2012) [arXiv:1207.6654 [astro-ph.CO]].
- [17] J. D. Bowman, A. E. E. Rogers, R. A. Monsalve, T. J. Mozdzen and N. Mahesh, *Nature* **555**, no. 7694, 67 (2018).
- [18] R. Hills, G. Kulkarni, P. D. Meerburg and E. Puchwein, arXiv:1805.01421 [astro-ph.CO].
- [19] R. Barkana, *Nature* **555**, no. 7694, 71 (2018) [arXiv:1803.06698 [astro-ph.CO]].
- [20] J. B. Muñoz and A. Loeb, arXiv:1802.10094 [astro-ph.CO].
- [21] A. Fialkov, R. Barkana and A. Cohen, arXiv:1802.10577 [astro-ph.CO].
- [22] Z. Kang, arXiv:1803.04928 [hep-ph].
- [23] A. Falkowski and K. Petraki, arXiv:1803.10096 [hep-ph].

- [24] G. Lambiase and S. Mohanty, arXiv:1804.05318 [hep-ph].
- [25] L. B. Jia, arXiv:1804.07934 [hep-ph].
- [26] P. Sikivie, arXiv:1805.05577 [astro-ph.CO].
- [27] A. Berlin, D. Hooper, G. Krnjaic and S. D. McDermott, arXiv:1803.02804 [hep-ph].
- [28] R. Barkana, N. J. Outmezguine, D. Redigolo and T. Volansky, arXiv:1803.03091 [hep-ph].
- [29] T. R. Slatyer and C. L. Wu, arXiv:1803.09734 [astro-ph.CO].
- [30] A. Ewall-Wice, T. C. Chang, J. Lazio, O. Dore, M. Seiffert and R. A. Monsalve, arXiv:1803.01815 [astro-ph.CO].
- [31] S. Fraser *et al.*, arXiv:1803.03245 [hep-ph].
- [32] Y. Yang, arXiv:1803.05803 [astro-ph.CO].
- [33] M. Pospelov, J. Pradler, J. T. Ruderman and A. Urbano, arXiv:1803.07048 [hep-ph].
- [34] K. Lawson and A. R. Zhitnitsky, arXiv:1804.07340 [hep-ph].
- [35] T. Moroi, K. Nakayama and Y. Tang, arXiv:1804.10378 [hep-ph].
- [36] D. Aristizabal Sierra, and C. S. Fong, arXiv:1805.02685 [hep-ph].
- [37] A. A. Costa, R. C. G. Landim, B. Wang and E. Abdalla, arXiv:1803.06944 [astro-ph.CO].
- [38] J. C. Hill and E. J. Baxter, arXiv:1803.07555 [astro-ph.CO].
- [39] C. Li and Y. F. Cai, arXiv:1804.04816 [astro-ph.CO].
- [40] G. D'Amico, P. Panci and A. Strumia, arXiv:1803.03629 [astro-ph.CO].
- [41] M. Safarzadeh, E. Scannapieco and A. Babul, arXiv:1803.08039 [astro-ph.CO].
- [42] S. Clark, B. Dutta, Y. Gao, Y. Z. Ma and L. E. Strigari, arXiv:1803.09390 [astro-ph.HE].
- [43] K. Cheung, J. L. Kuo, K. W. Ng and Y. L. S. Tsai, arXiv:1803.09398 [astro-ph.CO].
- [44] A. Hektor, G. Hutsi, L. Marzola, M. Raidal, V. Vaskonen and H. Veermae, arXiv:1803.09697 [astro-ph.CO].
- [45] H. Liu and T. R. Slatyer, arXiv:1803.09739 [astro-ph.CO].

- [46] A. Mitridate and A. Podo, arXiv:1803.11169 [hep-ph].
- [47] A. Schneider, arXiv:1805.00021 [astro-ph.CO].
- [48] A. Lidz and L. Hui, arXiv:1805.01253 [astro-ph.CO].
- [49] A. Hektor, G. Hütsi, L. Marzola, and V. Vaskonen, arXiv:1805.09319 [hep-ph].
- [50] J. B. Muñoz, C. Dvorkin and A. Loeb, arXiv:1804.01092 [astro-ph.CO].
- [51] A. A. Kaurov, T. Venumadhav, L. Dai and M. Zaldarriaga, arXiv:1805.03254 [astro-ph.CO].
- [52] M. Sitwell, A. Mesinger, Y. Z. Ma and K. Sigurdson, Mon. Not. Roy. Astron. Soc. **438**, no. 3, 2664 (2014) [arXiv:1310.0029 [astro-ph.CO]].
- [53] S. A. Wouthuysen, Astron. J. **57**, 31 (1952).
- [54] G. B. Field, Proc. IRE **46**, 240 (1958).
- [55] G. B. Field, Astrophys. J. **129**, 536 (1959).
- [56] S. Furlanetto, S. P. Oh and F. Briggs, Phys. Rept. **433**, 181 (2006) [astro-ph/0608032].
- [57] J. R. Pritchard and A. Loeb, Rept. Prog. Phys. **75**, 086901 (2012) [arXiv:1109.6012 [astro-ph.CO]].
- [58] A. Mesinger and S. Furlanetto, Astrophys. J. **669**, 663 (2007) [arXiv:0704.0946 [astro-ph]].
- [59] A. Mesinger, S. Furlanetto and R. Cen, Mon. Not. Roy. Astron. Soc. **411**, 955 (2011) [arXiv:1003.3878 [astro-ph.CO]].
- [60] Zahn, O., Mesinger, A., McQuinn, M., et al. Mon. Not. Roy. Astron. Soc. , 414, 727 (2011) arXiv:1003.3455 [astro-ph.CO].
- [61] Santos, M. G., Ferramacho, L., Silva, M. B., Amblard, A., & Cooray, A. , Mon. Not. Roy. Astron. Soc. , 406, 2421 (2010) arXiv:0911.2219 [astro-ph.CO].
- [62] Fialkov, A., Barkana, R., Pinhas, A., & Visbal, E. , Mon. Not. Roy. Astron. Soc. , 437, L36 (2014) arXiv:1306.2354 [astro-ph.CO].
- [63] Ross, H. E., Dixon, K. L., Iliev, I. T., & Mellema, G. , Mon. Not. Roy. Astron. Soc. , 468, 3785 (2017) arXiv:1607.06282 [astro-ph.CO].
- [64] Semelin, B., Eames, E., Bolgar, F., & Caillat, M. , Mon. Not. Roy. Astron. Soc. , 472, 4508 (2017) arXiv:1707.02073 [astro-ph.CO].

- [65] Z. Haiman, T. Abel and M. J. Rees, *Astrophys. J.* **534**, 11 (2000) [astro-ph/9903336].
- [66] R. J. Bouwens *et al.*, *Astrophys. J.* **803**, no. 1, 34 (2015) [arXiv:1403.4295 [astro-ph.CO]].
- [67] B. Greig and A. Mesinger, *Mon. Not. Roy. Astron. Soc.* **449**, no. 4, 4246 (2015) [arXiv:1501.06576 [astro-ph.CO]].
- [68] R. C. Livermore, M. Trenti, L. D. Bradley, S. R. Bernard, B. W. Holwerda, C. A. Mason and T. Treu, *Astrophys. J.* **861**, no. 2, L17 (2018) [arXiv:1805.05038 [astro-ph.GA]].
- [69] J. P. Gardner *et al.*, *Space Sci. Rev.* **123**, 485 (2006) [astro-ph/0606175].
- [70] J. Dalcanton *et al.*, arXiv:1507.04779 [astro-ph.IM].
- [71] Postman, M., Traub, W. A., Krist, J., et al. 2010, *Pathways Towards Habitable Planets*, 430, 361
- [72] B. Greig, and A. Mesinger, *Mon. Not. Roy. Astron. Soc.* **472**, 2651 (2017) [astro-ph/1705.03471].
- [73] S. Witte, P. Villanueva-Domingo, S. Gariazzo, O. Mena and S. Palomares-Ruiz, arXiv:1804.03888 [astro-ph.CO].
- [74] N. Aghanim *et al.* [Planck Collaboration], arXiv:1807.06209 [astro-ph.CO].
- [75] Y. Akrami *et al.* [Planck Collaboration], arXiv:1807.06211 [astro-ph.CO].